Published in final edited form as:
Angew Chem Int Ed Engl. 2019 January 28; 58(5): 1334–1339. doi:10.1002/anie.201810522.

Efficient Hyperpolarization of U-^{13}C-Glucose using Narrow-line UV-generated Labile Free Radicals

Dr Andrea Capozzi[#*,a], **Saket Patel, MSc**[#b], **Dr Christine Pepke Gunnarsson, MSc**[a], **Irene Marco-Rius**[c], **Dr Arnaud Comment**[c,d], **Dr Magnus Karlsson, MSc**[a], **Dr Mathilde H. Lerche**[a], **Dr Olivier Ouari**[b], and **Prof Jan Henrik Ardenkjær-Larsen**[a]

[a]Center for Hyperpolarization in Magnetic Resonance, Department of Electrical Engineering, Technical University of Denmark, Building 349, 2800 Kgs Lyngby (Denmark)

[b]Institut de Chimie Radicalire, Aix-Marseille Université, CNRS, ICR UMR 7273, 13397 Marseille Cedex 20 (France)

[c]Cancer Research UK Cambridge Institute, University of Cambridge, Li Ka Shing Centre, Cambridge (United Kingdom)

[d]General Electric Healthcare, Chalfont St Giles, Buckinghamshire HP8 4SP (United Kingdom)

[#] These authors contributed equally to this work.

Abstract

Free radicals generated via irradiation with UV-light of a frozen solution containing a fraction of pyruvic acid (PA), have demonstrated their dissolution Dynamic Nuclear Polarization (dDNP) potential providing up to 30% [1-^{13}C]PA liquid-state polarization. Moreover, their labile nature has proven to pave a way to nuclear polarization storage and transport. Herein, differently from the case of PA, we tackled the issue of providing dDNP UV-radical precursors, trimethylpyruvic acid (TriPA) and its methyl-deuterated form d_9-TriPA, not involved in any metabolic pathway. The ^{13}C dDNP performance, were evaluated for hyperpolarization of [U-$^{13}C_6$,1,2,3,4,5,6,6-d_7]-D-glucose. The generated UV-radical proved to be a versatile and highly efficient polarizing agent providing, after dissolution and transfer (10 s), a ^{13}C liquid-state polarization up to 32%.

Keywords

dissolution DNP; ESR spectroscopy; hyperpolarized glucose; NMR spectroscopy; UV-radicals

During the last decade, ^{13}C hyperpolarized (HP) magnetic resonance imaging (MRI) and spectroscopy (MRS) have encountered a tremendous development, showing convincing demonstrations in detecting and monitoring biochemical changes in real time in both clinical and preclinical studies.[1] Among the different hyperpolarization techniques used to increase the NMR sensitivity of the substrate, dissolution Dynamic Nuclear Polarization

[*] andcapo@electro.dtu.dk; Homepage: www.hypermag.dtu.dk.

Conflict of interest

Dr. Arnaud Comment is currently employed by General Electric Medial System, Inc.

Europe PMC Funders Author Manuscripts

(dDNP) is the most widespread one, because of its versatility in biomedical applications.[2] In particular, hyperpolarization of ^{13}C enriched molecules shows a combination of features that make it the ideal nucleus for real-time metabolic studies:[3] ubiquitous presence in biomolecules, large chemical shift dispersion (possibility to easily distinguish between several substrates), low natural abundance (absence of a background signal) and relatively long nuclear longitudinal relaxation time (T_{1n}) at specific molecular positions (e.g. carbonyl groups, tens of seconds). Indeed in a dDNP experiment, enhancement of the nuclear polarization (i.e. the relative difference between the populations of the two spin eigenstates) takes place *ex-situ* in the so-called DNP polarizer. The latter provides a moderate magnetic field (3.35 – 7 T) and a cold environment (1 – 1.5 K) hosting a glassy frozen sample that includes the substrate of interest (at molar concentration) and unpaired electrons (15 - 50 mM), in the form of organic free radicals. After the microwaves driven polarization transfer from the electron spins to the surrounding nuclear spins reaches a steady-state, the frozen sample is quickly dissolved in a hot buffer and ejected from the polarizer.[2b] Extracting the sample in the liquid state is at the same time the strength and weakness of the technique. On the one hand, the polarization created in the solid state is preserved, generating a high sensitivity metabolic probe ready to be injected. But on the other, a dedicated polarizer is needed as close as possible to the MRI scanner, since the HP state is T_{1n}-limited. A way to circumvent this limitation is to employ labile radicals.

Labile radicals, generated via irradiation with UV-light of a frozen solution containing a fraction of PA (UV-PA), have demonstrated their dDNP capability on PA itself and other substrates,[4] providing up to 30% [1-^{13}C]PA liquid-state polarization at optimal conditions.[5] Moreover, their unique feature to recombine around 190 K allows recovery of a HP solution without radicals, and has proven to pave the way, together with other approaches,[6] to nuclear polarization storage and transport. Indeed, quenching the radicals when the sample is still frozen improves the possibly of extracting it from the DNP polarizer and dissolve the HP sample far away from its production site.[7]

In the present work we tackled the issue of providing dDNP UV-radical precursors not involved in any metabolic pathway and producing labile radicals with improved ^{13}C dDNP performance compared to UV-PA. To this end, we investigated the photochemical properties of two α-keto acids, trimethylpyruvic acid (TriPA) and its methyl-deuterated form d_9-TriPA (see Figure 1). We studied their dDNP efficiency as non-persistent radicals on isotope labelled D-glucose ($^{13}C_6$,1,2,3,4,5,6,6-d_7), a substrate showing increasing interest in the hyperpolarization community thanks to the richer metabolic pathways it can give access to, compared to the routinely used [1-^{13}C]pyruvate.[8]

Narrow ESR-line radicals (e.g. Trityls or BDPA), are well known to provide good direct DNP enhancements on ^{13}C nuclei.[9] Although UV-PA has a thinner spectrum than the well-known broad nitroxyl radicals (e.g. TEMPO and TEMPOL), it still shows an ESR-line too broad compared to the ^{13}C Larmor frequency, providing efficient DNP on protons. Thus, it may not be the optimal structure for direct ^{13}C nuclei polarization.[4a]

The generation of labile paramagnetic species from UV-light illumination of α-keto acids has been explained by photoexcitation of the $n - \pi^*$ transition (300 – 350 nm) of the α-

carbonyl group, followed by efficient intersystem crossing (ISC) to an excited triplet state (^{3}PA*).[10] When PA is the photoactive precursor, ^{3}PA* can react with another PA molecule and two paramagnetic intermediates are expected to appear: the ketyl radical CH3Ċ(OH)C(O)OH (R1 in Figure 1) and the acyloxyl radical CH3C(O)C(O)Ȯ (R2 in Figure 1); the latter can then decarboxylates into the acetyl radical CH3ĊC(O).[11] These radicals are extremely unstable at room temperature, but can be, at least partially, “captured” when the UV-irradiation takes place in liquid nitrogen (77 K).[12] Having a clear understanding of which intermediates survive is crucial for the appropriate choice or chemical synthesis of UV-radical precursors with improved ^{13}C dDNP properties. To clarify this point UV-irradiation was performed in liquid nitrogen on frozen solutions of glycerol:water 50:50 (v/v) (GW55) containing 10% of natural abundance PA or PA with site specific ^{13}C labelling.

In Figure 2A to 2C, the X-band ESR spectrum measured at 77 K (black line) and the corresponding fit (dashed red line) are reported for UV-irradiated PA:GW55 1:9 (v/v), [1-^{13}C]PA:GW55 1:9 (v/v) and [2-^{13}C]PA:GW55 1:9 (v/v), respectively. While the same g-tensor = [2.0036 2.0027 2.0007] could be used for fitting all three spectra, it is interesting to see how the hyperfine coupling changes as a function of the ^{13}C labelling of the PA molecule. In panel A the peak quartet spectrum was reproduced through an isotropic coupling a_{1H} = 1.67 mT to the magnetically equivalent methyl protons, in good agreement with previous studies.[12] In panel B the ^{13}C labelling in C1 position generated a peak quintet and it was taken into account by adding an extra isotropic coupling a_{13C} = 1.07 mT. In panel C the strong (a_{13C} = 2.82 mT) coupling to the ^{13}C nucleus in C2 position changed dramatically the ESR spectrum appearance generating almost a doublet of quartet (for more details about spectra fitting see Supporting Information). Thus, ^{13}C labelling affected the spectrum in both cases with a stronger effect on C2. On the basis of the foregoing discussion, we can state that the radical stabilized by the cold environment and thus, active DNP wise is the ketyl one. It appears clear now that the choice of TriPA as UV-radical precursor provides a more isolated electron environment: by pushing the methyl protons two carbon positions away, the hyperfine coupling was reduced (a_{1H} = 0.11 mT) generating a sharp single line X-band ESR spectrum (see Figure 2D). Deuteration of the methyl groups decreased the hyperfine coupling (a_{2H} = 0.02 mT) and the ESR linewidth even further (data not shown). Moreover, the g-anisotropy was less pronounced when TriPA and d9-TriPA were the radical precursors: g-tensor = [2.0031 2.0022 2.0012] (see Supporting Information for spectra comparison at 6.7 T).

As previously described,[5] also UV-irradiated dDNP samples were prepared in liquid nitrogen outside from the polarizer. We studied frozen solutions consisting of 0.7 M TriPA and d_9-TriPA with 2 M [U-^{13}C,d_7]glucose dissolved in GW55. From now onward the two preparations will be addressed as *TriPA_DNP-sample* and *d_9-TriPA_DNP-sample*, respectively. Aiming at minimizing as much as possible the precursor molecules amount in the sample, the chosen concentration (corresponding to 10% of the final volume) was the lowest providing enough radical to perform efficient DNP at 6.7 T and 1.1 K for both samples (see Supporting Information). In Figure 3A the radical generation as a function of UV-irradiation time is reported. In both cases irradiating for 300 s was sufficient to reach the radical concentration plateau. Surprisingly the radical yield was doubled when d_9-TriPA was

employed. For the sake of comparison a third sample containing 0.7 M of PA was prepared. The latter generated half of the radical concentration obtained with the TriPA sample. We found experimental evidence that the TriPA light absorption in correspondence to the $n - \pi^*$ transition was approximately half as strong as d_9-TriPA and twice as strong as PA (Figure 3B). This observation together with the fact that, for a given precursor concentration, the radical yield is strictly UV-light power dependent[5] may explain the behaviour reported in Figure 3A. Another possible explanation, or confounding factor, could be related to the different amount of precursor in the hydrate form. Indeed, when in water solution, hydration of the carbonyl group of ketones is a well-known phenomenon.[11] The hydrate form of the precursor molecule is not photoactive and does not contribute to the generation of any radical.[13] We estimated the amount of trimethylpyruvate, d_9-trimethylpyruvate and pyruvate hydrate in the three liquid mixtures via ^{13}C NMR. A higher amount of hydrate characterized the sample containing PA, but no significant difference in hydrate amounts was observed between the other two (Supporting Information). Although beyond the scope of the present work, the physical chemistry behind the origin of the isotopic effect characterizing d_9-TriPA remains unclear.

In order to obtain efficient DNP, it is important to achieve a homogenous radical distribution inside the frozen sample. This is a minor issue when using chemical doping,[14] but may be more challenging when radicals are photo-induced. Using a methodology previously described,[5] we demonstrated that for this low concentration of precursor the paramagnetic centres were homogeneously induced inside the sample volume (see Supporting Information).

In Figure 4 the ESR spectrum and ^{13}C DNP microwaves sweep measured at 6.7 T and 1.1 K are shown for *TriPA_DNP-sample* and *d_9-TriPA_DNP-sample*. Even at high field, where the anisotropic Zeeman interaction dominates the linewidth,[15] the deuterated sample showed a slightly narrower ESR spectrum (grey curves) because of the reduced hyperfine coupling to the methyl groups (numerical values are reported in Table 1). Nevertheless this feature did not generate any significant difference between the widths of the two ^{13}C DNP sweeps (blue curves). For both samples the maximum positive and negative DNP enhancement (DNP+ and DNP-) appeared at 187.98 GHz and 188.17 GHz, respectively, with |DNP-| > |DNP+|. Modulation of the microwaves frequency improved the DNP enhancement (red curve). A stronger effect was observed on the protonated sample: at optimal conditions (20 MHz of modulation amplitude, 1 kHz of modulation frequency), the DNP-value improved by 37% for *TriPA_DNP-sample* and 23% for *d_9-TriPA_DNP-sample*. This difference is in good agreement with the different radical concentration generated in the two samples. Indeed, a higher radical concentration yields stronger electron spin dipolar coupling. The latter, especially at high field, represents a key parameter to efficiently saturate the radical ESR line and provide better DNP performance, thus decreasing the microwaves modulation effect.[16] By modulating the microwave frequency a beneficial effect was observed already at a rate of 10 Hz, in good agreement with the electron spin-lattice relaxation time (T_{1e}), estimated to be approximately 100 ms (see Supporting Information). The best DNP enhancement was achieved with 1 kHz modulation rate of the microwave frequency, and all polarization values herein reported were obtained at these experimental conditions.

TriPA_DNP-sample and *d_9-TriPA_DNP-sample* were polarized at optimal conditions (microwaves frequency 188.19 GHz with ±20 MHz frequency modulation at a rate of 1 kHz) to estimate the maximum achievable DNP enhancement. The build-up time constants (T_b) were 1836±28 s and 1230±30 s, respectively (n=3). Once at the plateau the samples were quickly dissolved and transferred (T_{trans} = 10 s) to a 9.4 T high resolution magnet kept at 40 °C (see Figure 5). The ^{13}C liquid-state polarization (*PLS*) was be 26.8±1.1 % for *TriPA_DNP-sample* and 30.1±1.8 % for *d_9-TriPA_DNP-sample*; in both cases the liquid state T_{1n} was close to 20 s (n = 3). Because of the excessively long spin-lattice relaxation time in the solid state (>13 h), the polarization value at the moment of dissolution (P_{SS}) was measured only once for each sample. The result was in good agreement with the value back calculated from the liquid-state polarization: $P_{SS} = P_{LS} \cdot exp(T_{trans}/T_{1n})$. We obtained solid-state polarizations of 42.9±1.8 % and 49.5±3.0 % for *TriPA_DNP-sample* and *d_9-TriPA_DNP-sample*, respectively. To test the versatility and improved DNP performance of the new UV-radicals we polarized the reference substrate 1,1-bis(hydroxymethyl)cyclopropane-1-^{13}C,d_8 (HP001), at the same DNP conditions of *d_9-TriPA_DNP-sample* where 2 M HP001 replaced the labelled glucose in the preparation. HP001 is a well suited “polarization probe” since its liquid state T_{1n} = 123.0±1.0 s. The measured ^{13}C liquid-state polarization of HP001 was 53.7±2.0 % (n = 2) (see supporting Information).

We compared the results achieved using UV-TriPA and UV-d_9-TriPA to the routinely used trityl radical. The *Trityl_DNP-sample* was prepared by dissolving 30 mM trityl radical AH111501 and 2 M labelled glucose in GW55, and irradiating with microwaves at 187.94 GHz corresponding to DNP+ for trityl (see Supporting Information). Although 30 mM trityl radical represents the optimal concentration to perform dDNP on [1-^{13}C]PA at 6.7 T (with 70% ^{13}C polarization routinely obtained),[17] *Trityl_DNP-sample* liquid-state polarization was not any higher than 21.1±1.5 % (n = 3) in good agreement with previous results.[8a] All relevant dDNP data are summarized in Table 1.

We verified the radicals persistency in vision of establishing a robust protocol for storage and transport of HP glucose samples.[7] In Figure 6 we report how the UV-TriPA (panel A) and UV-d_9-TriPA respond to temperature. In order to compensate for the Boltzmann factor and take into account the number of paramagnetic centres only, the ESR signal intensity multiplied by the temperature was plotted as a function of the latter. The characteristic “step function” profile clearly shows that all radicals are suddenly quenched above 190 K. Thus, the samples became diamagnetic when still frozen.

We finally injected the UV-TriPA hyperpolarised [U-^{13}C,d7]glucose into live prostate carcinoma cells to judge the spectral influence of the presence of radical precursor (see Figure 7). At the current concentration the signals from the precursor are clearly large relative to the metabolite signals in a cell experiment with limiting biological material (7 million cells). However, none of the precursor signals overlap with metabolites from the glycolysis and has thus no influence on a kinetic analysis.

The results herein show that UV-TriPA and UV-d_9-TriPA, are valuable polarizing agents for ^{13}C DNP at high magnetic field. Compared to UV-PA, they benefit from a higher radical

yield and improved DNP performance. These two features, respectively, are a consequence of stronger light absorption in correspondence to the n-π^* electron transition and a narrower ESR spectrum due to reduced g-anisotropy and hyperfine coupling to the C2 position. Indeed the ^{13}C polarization level achieved was comparable to or better than trityl radical for the same sample. Moreover, their unique property of quenching above 190 K has two main advantages: first it allows recovering a HP solution naturally free of radical; second and more important, it represents the key feature to move towards a protocol for polarization storage. Our next aim is to decrease the radical precursor concentration to the tens of mM range, in order to reduce as much as possible the presence of any liquid-state background signal other than the HP substrate itself in a metabolic study. Preliminary results show that by doubling the irradiation power by using two sources simultaneously, it is possible to achieve the same radical concentration with half of the precursor amount. Indeed, as shown in Figure 3B the overlap between the irradiance of the UV-source and the absorbance of TriPA and d_9-TriPA is relatively small. As recently demonstrated, efficient photo-generation of these labile radicals is strictly related to the photon density at the radical precursor light absorption peak.[18]

Experimental Section

Chemicals were purchased from Sigma-Aldrich, (2605 Brøndby, Denmark) excepted for the radical precursor d_9-TriPA (synthesized in house, see Supporting Information) and the Trityl radical AH111501 (GE Healthcare, 01494 Amersham, UK). All experimental methods and hardware used were described previously.[5]

The UV-source (Dymax, BlueWave 75) spectral irradiance was kindly provided by the manufacturer. In the present work the UV-source was always operated at its maximum power (19 W/cm^2). Indeed, as previously demonstrated for the case of PA,[5] the maximum radical yield was achieved at these experimental conditions.

It is worth pointing out that the HP sample was finally dissolved in 10 ml of hot 40 mM phosphate buffer.

Supplementary Material

Refer to Web version on PubMed Central for supplementary material.

Acknowledgements

The research leading to these results has received funding from the Danish National Research Foundation (DNRF124); the European Union's Horizon 2020 research and innovation programme under the Marie Sklodowska-Curie grant agreement no. 713683 (COFUNDfellowsDTU); the Marie Skladowka-Curie ITN studentship under grant agreement No 642773 (EUROPOL).

References

[1]. a)Golman K, in't Zandt R, Thaning M. P Natl Acad Sci USA. 2006; 103:11270–11275.b)Nelson SJ, Kurhanewicz J, Vigneron DB, Larson PEZ, Harzstark AL, Ferrone M, van Criekinge M, Chang JW, Bok R, Park I, Reed G, et al. Sci Transl Med. 2013; 5:191–110. 198ra108.c)Ardenkjaer-Larsen JH, Boebinger GS, Comment A, Duckett S, Edison AS, Engelke

F, Griesinger C, Griffin RG, Hilty C, Maeda H, Parigi G, et al. Angew Chem Int Edit. 2015; 54:9162–9185.

[2]. a)Ardenkjaer-Larsen JH, Fridlund B, Gram A, Hansson G, Hansson L, Lerche MH, Servin R, Thaning M, Golman K. P Natl Acad Sci USA. 2003; 100:10158–10163.b)Ardenkjaer-Larsen JH. J Magn Reson. 2016; 264:3–12. [PubMed: 26920825]

3. Brindle KM. J Am Chem Soc. 2015; 137:6418–6427. [PubMed: 25950268]

[4]. a)Capozzi A, Hyacinthe JN, Cheng T, Eichhorn TR, Boero G, Roussel C, van der Klink JJ, Comment A. J Phys Chem C. 2015; 119:22632–22639.b)Eichhorn TR, Takado Y, Salameh N, Capozzi A, Cheng T, Hyacinthe JN, Mishkovsky M, Roussel C, Comment A. P Natl Acad Sci USA. 2013; 110:18064–18069.c)Bastiaansen JAM, Yoshihara HAI, Capozzi A, Schwitter J, Gruetter R, Merritt ME, Comment A. Magnet Reson Med. 2018; 79:2451–2459.

[5]. Capozzi A, Karlsson M, Petersen JR, Lerche MH, Ardenkjaer-Larsen JH. J Phys Chem C. 2018; 122:7432–7443.

[6]. a)Hirsch ML, Kalechofsky N, Belzer A, Rosay M, Kempf JG. J Am Chem Soc. 2015; 137:8428–8434. [PubMed: 26098752] b)Ji X, Bornet A, Vuichoud B, Milani J, Gajan D, Rossini AJ, Emsley L, Bodenhausen G, Jannin S. Nature Communications. 2017; 8

7. Capozzi A, Cheng T, Boero G, Roussel C, Comment A. Nat Commun. 2017; 8:15757. [PubMed: 28569840]

8. a)Mishkovsky M, Anderson B, Karlsson M, Lerche MH, Sherry AD, Gruetter R, Kovacs Z, Comment A. Sci Rep-Uk. 2017; 7b)Rodrigues TB, Serrao EM, Kennedy BWC, Hu DE, Kettunen MI, Brindle KM. Nat Med. 2014; 20:93. [PubMed: 24317119] c)Harris T, Degani H, Frydman L. Nmr Biomed. 2013; 26:1831–1843. [PubMed: 24115045] d)Meier S, Karlsson M, Jensen PR, Lerche MH, Duus JO. Mol Biosyst. 2011; 7:2834–2836. [PubMed: 21720636]

[9]. a)Lumata L, Merritt ME, Kovacs Z. Phys Chem Chem Phys. 2013; 15:7032–7035. [PubMed: 23552448] b)Lumata L, Merritt ME, Malloy CR, Sherry AD, Kovacs Z. J Phys Chem A. 2012; 116:5129–5138. [PubMed: 22571288]

[10]. a)Leermakers PA, Vesley GF. J Org Chem. 1963; 28:1160.b)Leermakers PA, Vesley GF. J Am Chem Soc. 1963; 85:3776.

[11]. Guzman MI, Colussi AJ, Hoffmann MR. J Phys Chem A. 2006; 110:3619–3626. [PubMed: 16526643]

[12]. Guzman MI, Colussi AJ, Hoffmann MR. J Phys Chem A. 2006; 110:931–935. [PubMed: 16419992]

[13]. Griffith EC, Carpenter BK, Shoemaker RK, Vaida V. Proc Natl Acad Sci U S A. 2013; 110:11714–11719. [PubMed: 23821751]

[14]. Weber EMM, Sicoli G, Vezin H, Frebourg G, Abergel D, Bodenhausen G, Kurzbach D. Angew Chem Int Edit. 2018; 57:5171–5175.

[15]. Weil JA, Anderson JH. J Chem Phys. 1961; 35:1410.

[16]. a)Wenckebach WT. J Magn Reson. 2017; 284:104–114. [PubMed: 29028542] b)Bornet A, Milani J, Vuichoud B, Linde AJP, Bodenhausen G, Jannin S. Chem Phys Lett. 2014; 602:63–67.

[17]. Ardenkjær-Larsen JH, Bowen S, Petersen JR, Rybalko O, Vinding MS, Ullisch M, Nielsen NC. Magnet Reson Med. 2018

[18]. Marco-Rius I, Cheng T, Gaunt AP, Patel S, Kreis F, Capozzi A, Wright AJ, Brindle KM, Ouari O, Comment A. J Am Chem Soc. 2018; 140:14455–14463. [PubMed: 30346733]

Europe PMC Funders Author Manuscripts

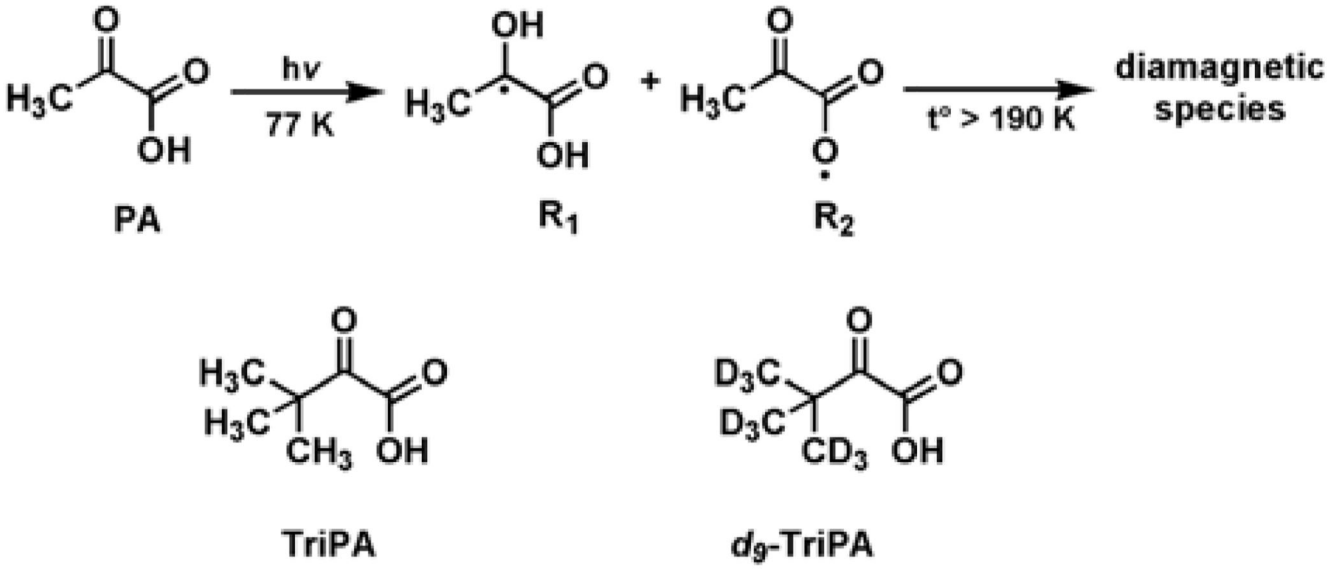

Figure 1.
Free radicals generated by UV-irradiation of PA and structures of TriPA and d9-TriPA.

Europe PMC Funders Author Manuscripts

Europe PMC Funders Author Manuscripts

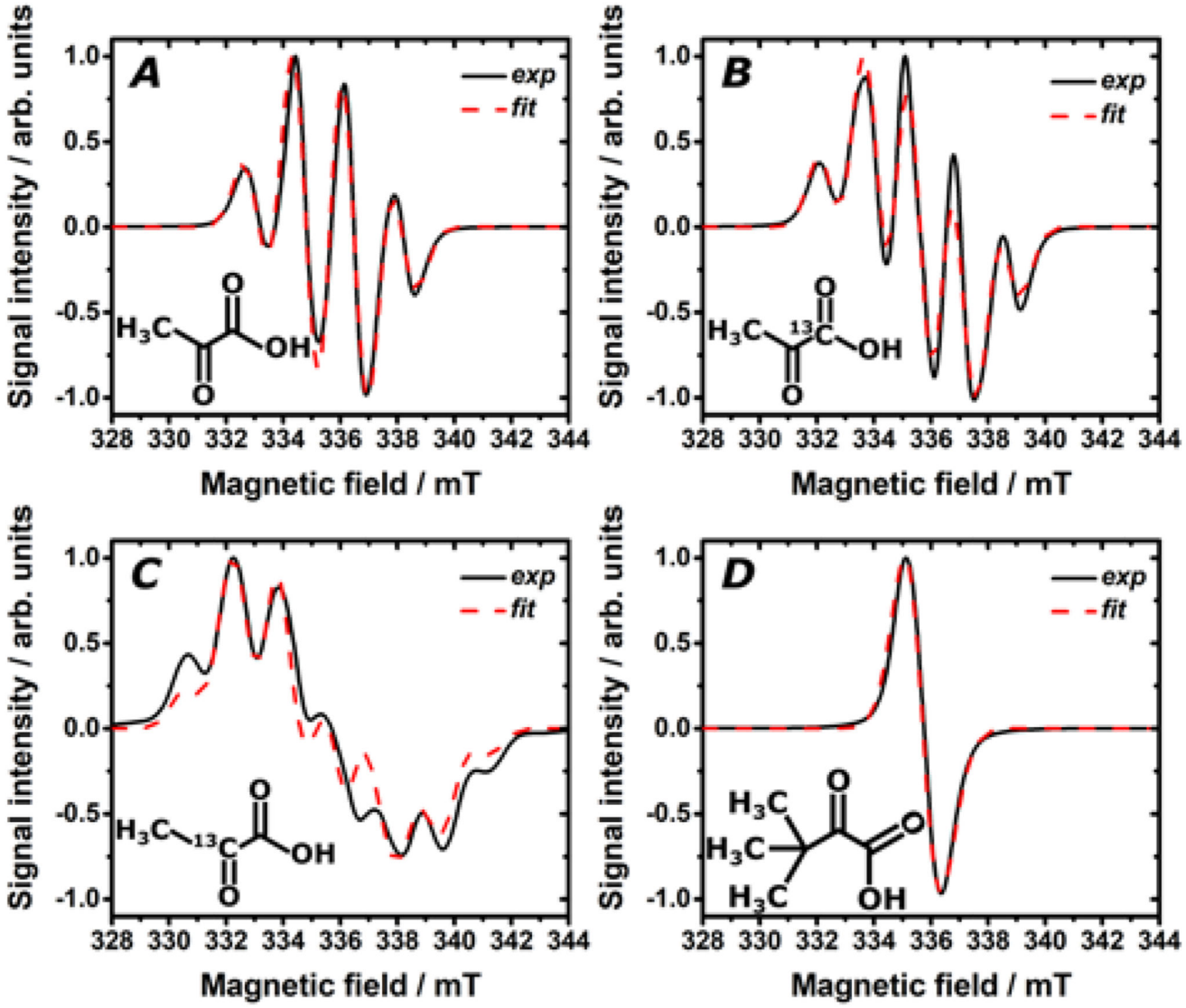

Figure 2.

X-band ESR measurement (black line) and ESR spectrum fit (dashed red line) after 5 min UV-light irradiation at 77 K of a single 4.0±0.2 μl bead of a frozen solution containing PA:GW55 1:9 (v/v) (**A**); [1-^{13}C]PA:GW55 1:9 (v/v) (**B**); [2-^{13}C]PA:GW55 1:9 (v/v) (**C**); TriPA:GW55 1:9 (v/v) (**D**). GW55 is an abbreviation for the solvent composition glycerol:water 50:50 (v/v). In the insert the structural formula of the radical precursor is shown.

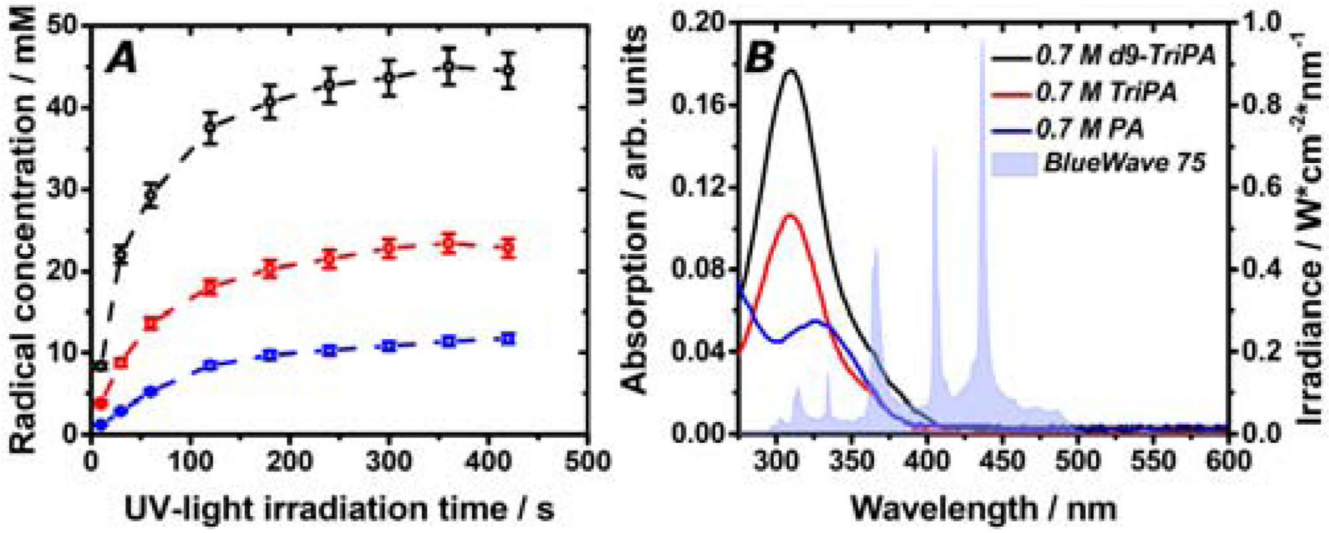

Figure 3.

Radical generation at 77 K as a function of UV-irradiation time for frozen mixtures of 0.7 M TriPA (red curve), d_9-TriPA (black curve) and PA (blue curve) with 2 M [U-^{13}C,d_7]-D-glucose dissolved in GW55. Measurements were performed on a single 4.0±0.2 μL frozen bead immersed in liquid nitrogen (**A**). Room temperature UV-vis absorption measurements for the same sample solutions (left y-scale); the light blue coloured area represents the spectral irradiance (right y-scale) of the UV-source (Dymax, BlueWave 75) at maximum power (19 W/cm^2) used to photo-generate the radicals (**B**).

Europe PMC Funders Author Manuscripts

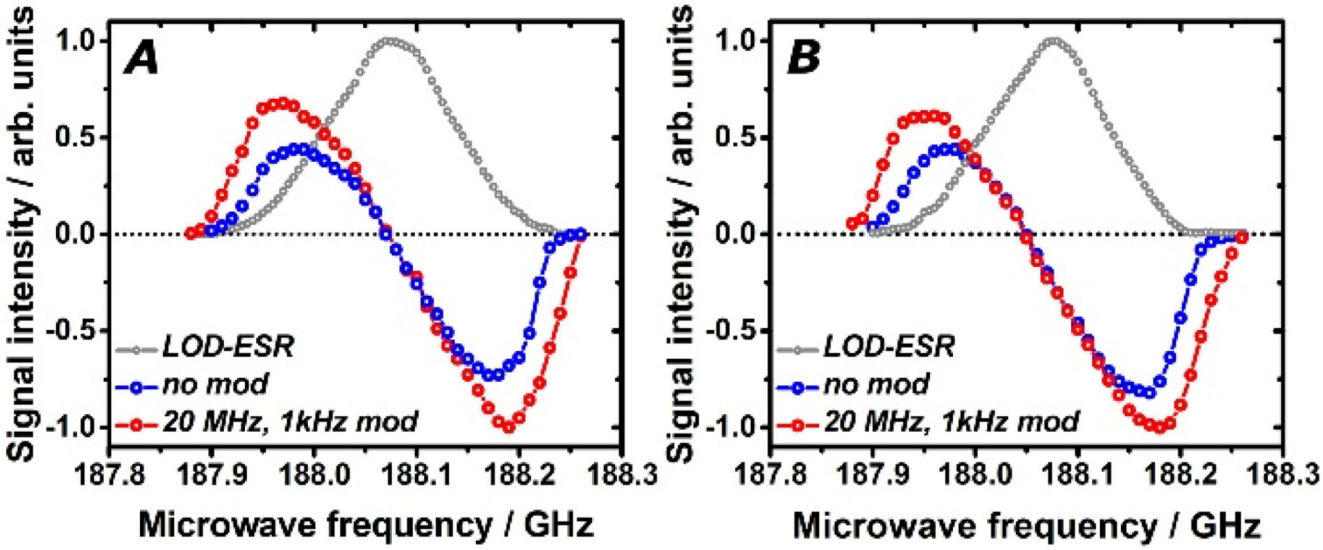

Figure 4.

The longitudinal detected (LOD) ESR spectrum (grey curve) and the ^{13}C DNP microwaves sweep without modulation (blue curve) and with modulation (red curve) are reported for *TriPA_DNP-sample* (panel **A**) and *d_9-TriPA_DNP-sample* (panel **B**). All measurements were performed at 6.7 T and 1.1 K. Samples were UV-irradiated in liquid nitrogen for 300 s.

Europe PMC Funders Author Manuscripts

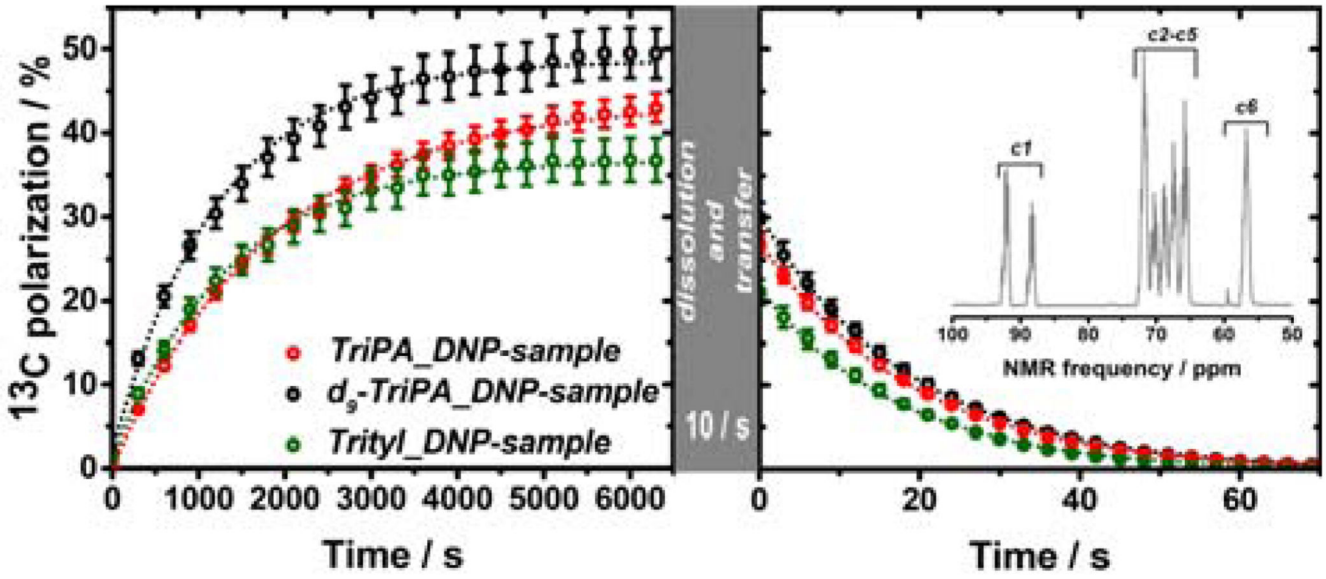

Figure 5.

The ^{13}C polarization solid-state build-up (left panel) and liquid-state relaxation (right panel) are showed for *TriPA_DNP-sample*, *d_9-TriPA_DNP-sample* and *Trityl_DNP-sample*. Solid-state measurements were performed at 6.7 T and 1.1 K by mw irradiation at 188.19 GHz (20 MHz amplitude modulation and 1 kHz frequency modulation) for *TriPA_DNP-sample* and *d_9-TriPA_DNP-sample*; *Trityl_DNP-sample* was polarized at the 187.94 GHz (no microwaves modulation) corresponding to the optimum for Trityl (see Supporting Information). Liquid-state measurements were acquired on 9.4 T high resolution magnet equipped with a 5 mm NMR probe kept at 40 °C. The transfer of the HP solution from the polarizer to the high resolution magnet took 10 s. In the inset the HP [U-^{13}C,d_7]-D-glucose NMR spectrum corresponding to the first point of *d_9-TriPA_DNP-sample* signal decay is reported (C2-C5 DNP enhancement = 41000).

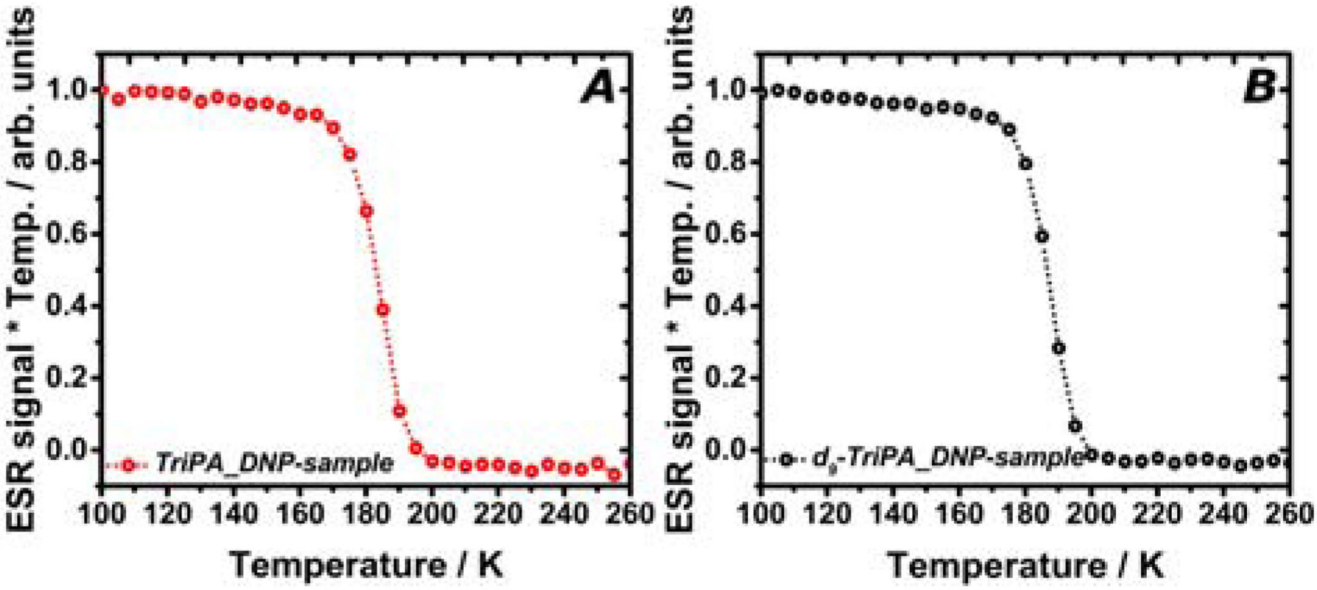

Figure 6.

The ESR signal as a function of temperature is reported for *TriPA_DNP-sample* (panel A) and *d_9-TriPA_DNP-sample* (panel B). In both cases, the ESR signal suddenly disappeared above 190 K. The two samples became diamagnetic when still frozen.

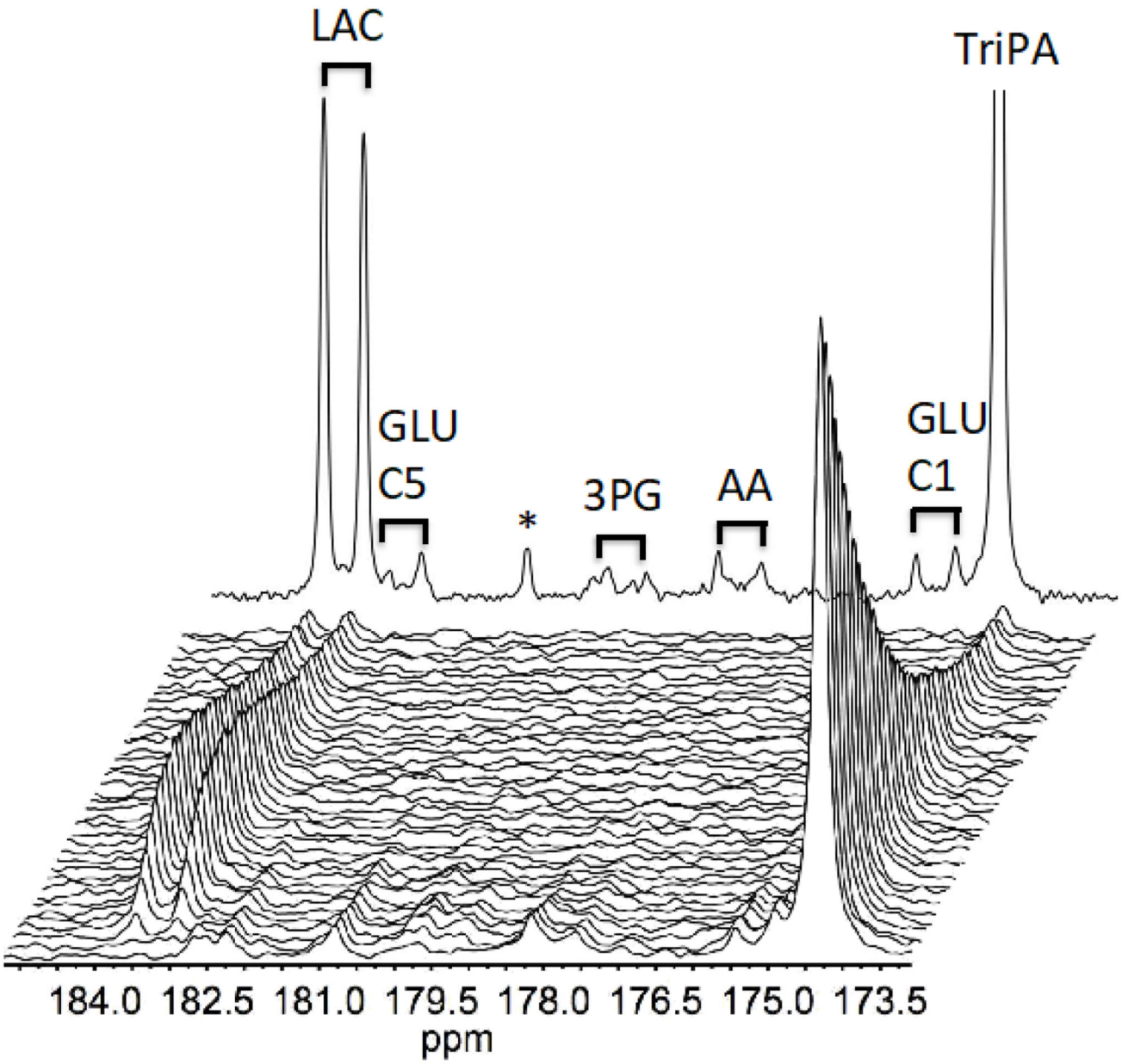

Figure 7.

UV-TriPA hyperpolarised [U-^{13}C,d_7]glucose conversion in live prostate carcinoma cells (PC-3). A build-up of the glycolysis derived metabolite lactate could be followed over 30 s. Intermediates in glycolysis are identified by ^{13}C-^{13}C coupling constants due to the uniformly labelled substrate and indicated by black bars in a sum of 30 spectra: Lactate (LAC), Glutamate carbon #1 and #5 (GLU-C1 and C5), 3-phophoglucerate (3PG), unspecified amino acid (AA). Remaining radical precursor is identified outside ppm area of interest as singlets (TriPA). The signal denoted * is likely to originate from the precursor.

Europe PMC Funders Author Manuscripts

Table 1

The main dDNP parameters and results obtained for *TriPA_DNP-sample*, *d_9-TriPA_DNP-sample* and *Trityl_DNP-sample* at 6.7 T and 1.1 K are summarized. From the 1st to 7th column we report in order: sample name, radical concentration, ESR spectrum full-width at half-maximum measured at DNP conditions, solid-state buildup time constant T_b, solid-state back calculated ^{13}C polarization, liquid-state ^{13}C polarization and liquid-state relaxation time T_{1n}.

DNP Sample	*Radical conc [mM]*	*ESR linewidth [MHz]*	*SS T_b [s]*	*SS pol [%]*	*LS pol [%]*	*LS T_{1n} [s]*
TriPA	20±1	142	1836±28	49.5±3.0	30.1±1.8	20.1±1.0
d9-TriPA	40±1	131	1230±30	42.9±2.8	26.8±1.1	19.8±1.0
Trityl_DNP	30	108	1330±28	35.7±2.5	21.1±1.5	19.4±0.8